Prediction of Austenitic Weld Metal Microstructure and Properties

With advent of new stainless steels, a wider range of alloys must be considered in predicting ferrite

BY D. L. OLSON

ABSTRACT. Diagrams, such as the Schaeffler and DeLong diagrams, have been used to assist in the proper selection and use of austenitic filler materials and to predict weld metal microstructures and properties. These diagrams have been very successful in predicting the amount of delta ferrite in stainless steel weld metal. This paper is concerned with the predictability of austenitic weld metal microstructure and properties over a larger compositional range.

There are two main different types of phase transformations associated with austenitic weld metal. Existing analytical methodology has been successful at predicting quantitatively the nature of the liquid to delta ferrite transformation. But the austenite to martensite transformation for high alloy weld metal needs to be better understood if welding consumables for new high manganese ferrous alloys are to be developed to achieve optimum properties and service behavior. In this paper, new expressions are introduced to predict the martensite start room temperature composition or the martensite start temperature. Some of these high manganese ferrous alloys are the basis for the new "no chromium" stainless steel. Various available diagrams, which allow for the prediction of weld metal microstructure, will be given.

New mathematical forms for expressions to predict weld metal phase stability and microstructure, based on solution thermodynamics and kinetics, will be introduced. These new expressional forms should allow for better predictability over a larger alloy range. The non-homogeneous (cored) nature of the weld metal composition will also be considered. These new forms can allow fundamental alloying and solid solution information to be obtained from the microstructure or property correlations with the weld metal compositions.

Introduction

As new engineering materials are developed it is important to develop the methods and materials for welding them. Austenitic weld metals are frequently utilized for joining various engineering materials and for a variety of reasons. Austenitic consumables have been extensively used to form the transition weld metal in dissimilar ferrous alloy joints, to join stainless steel, in weld repair, in hardfacing, and in corrosion resistant claddings. If properly alloyed, austenitic weld metal is strong, ductile, resistant to hot-cracking, and capable of retaining potentially troublesome contaminants in solid solution. Austenitic consumable wire is readily cold formed, facilitating its production. But some austenitic compositions are characterized by a high thermal expansion coefficient which often leads to the development of high residual stresses in the weld. Weld metal microstructures based on traditional austenitic weld metal compositions can be predicted from empirical diagrams, such as the Schaeffler diagram (Ref. 1). Difficulties arise, however, when the weld metal composition extends beyond the application range of the original empirical relationships. This situation is the case, for instance, when the Schaeffler diagram is applied to weld metal of a different thermal history, or of a vastly different chromium concentration, than that of the original study. It would, therefore, be advantageous to utilize the fundamentals of materials science to develop expressions which would be more generally applicable to predict weld metal microstructure and properties.

The Fe-Cr-Ni Weld Metal System

In 1906 Guillet (Ref. 2) first introduced the Fe-Cr-Ni alloy system as a potential engineering material for corrosion resistance and mechanical applications. The works of Gieson (Ref. 3), Monnartz (Ref. 4), and Maurer and Strauss (Ref. 5) led to the commercialization of the 18Cr-8Ni alloys, the basis for most of the 300 series stainless steel alloys. By 1934, the understanding that low carbon contents (0.03) gave austenitic stainless steel a superior intergranular corrosion resistance was established.

Strauss and Maurer (Ref. 6) introduced a nickel-chromium diagram, which was later modified by Scherer, Riedrich and Hoch (Ref. 7), that allowed prediction of the various phases in the microstructure

This paper is the 1984 Adams Lecture, presented at the AWS 65th Annual Meeting, held April 9-13, 1984, in Dallas, Tex.

D. L. OLSON is Professor and Director at the Center for Welding Research, Colorado School of Mines, Golden, Colo.

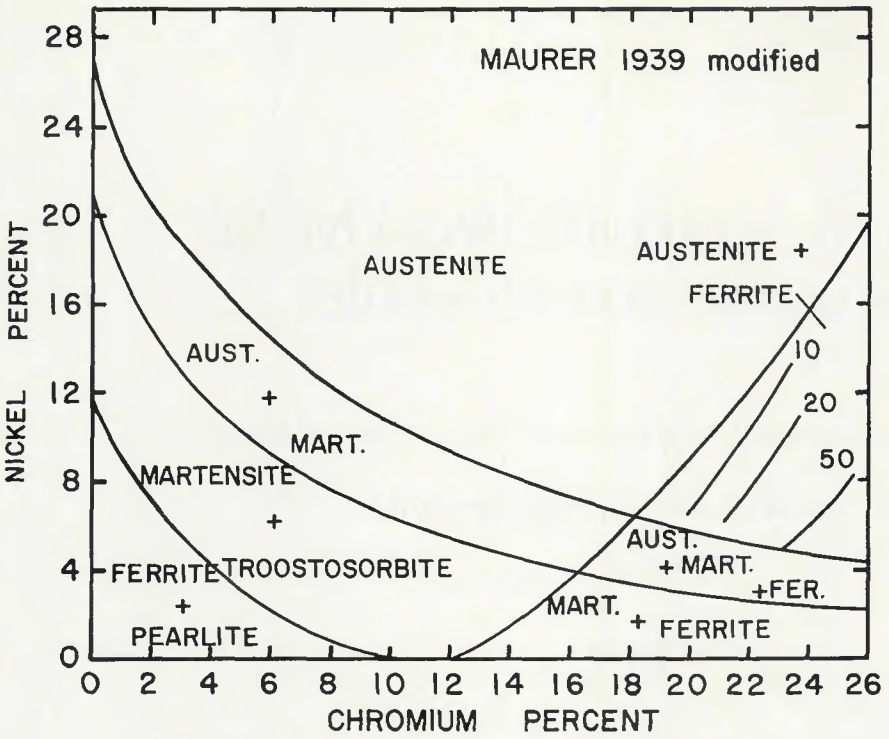

Fig. 1 – The nickel-chromium diagram used by Maurer to predict microstructure. Notice that the phase boundary lines are curved

within the composition range of 0 to 26 weight percent chromium and 0 to 25 weight percent nickel. If carbon, silicon and manganese contents were held within specific limits, the lines of this nickel-chromium diagram were useful in predicting microstructure for a given composition. The diagram had curved lines, as seen in Fig. 1, defining regions of austenite, ferrite, martensite, troostosorbite (very fine pearlite), and regions of combinations of these phases. The diagram was developed based on wrought materials and not solidified materials.

Newell and Fleischmann (Ref. 8) were first in developing an expression for defining austenite stability as a function of alloy content for this system. They were also concerned with wrought product. Their constituitive expression for predicting the austenite-austenite plus ferrite boundary is given as:

$$Ni = \frac{(Cr + 2Mo - 16)^2}{12} - \frac{Mn}{2} + 30\,(0.10 - C) + 8 \qquad (1)$$

where the chemical symbols represent weight percent of that element. Notice in the Newell-Fleischmann equation that manganese is reported to be one-half as effective in stabilizing austenite as nickel. Carbon was reported to be 30 times more effective than nickel. Also, chromium and molybdenum were both found to have a nonlinear relationship with nickel, which is consistent with the curve line for the boundary for the austenite and austenite plus ferrite regions on the Maurer diagram – Fig. 1. The Newell-Fleischmann equation was reported to describe the austenite stability curve in the 14 to 19 percent chromium and the 10 to 16 percent nickel range.

The science of welding with austenite filler materials became a high interest topic just prior to and during World War II. Besides the need to produce quality stainless steel consumables, the activity in austenitic welding during this period had to do with welding high strength (armor) materials for the national defense efforts (Refs. 9–24). The use of austenitic weld metal in welding difficult ferrous assemblies was based on the knowledge obtained during the previous decade that austenitic stainless steel can maintain high ductility and moderate strength over a large temperature range with fairly wide compositional variations. What was required for proper application of Fe-Cr-Ni austenitic consumables was some quantitative method to predict the maximum amount of base metal dilution that can be realized and still achieve the weld metal composition which will produce a ductile austenitic matrix and not a brittle weld metal martensitic structure.

Feild, Bloom and Linnert (Ref. 10) applied the Newell-Fleischmann expression to predict weld metal microstructure and found that the expression did not accurately predict solidified microstructure. Their specific concern was in predicting austenitic weld metal microstructure that was being used to weld armor steel. They reported that the weld should contain some ferrite to assist in preventing root bead cracking. Feild, Bloom and Linnert (Ref. 10) reported that a modification to the Newell-Fleischmann expression, by changing the constant, 8, to 14 in equation 1, gave a better prediction of austenite stability for the compositional range where chromium varied from 18 to 21 percent and nickel varied 9 to 11 percent. Moving the austenite promoter to the left side, the expression becomes

$$Ni + 0.5Mn + 30C = \frac{(Cr + 2Mo - 16)^2}{12} + 14 \qquad (2)$$

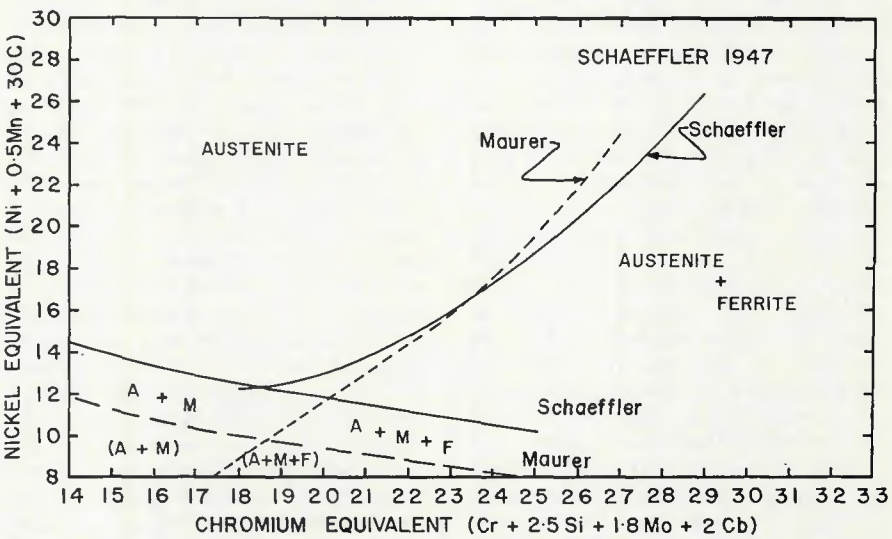

Fig. 2 – The Schaeffler diagram of 1947, which indicates some of the primary phase boundaries, compares the curve from Maurer's nickel-chromium diagram to the Schaeffler diagram which uses nickel and chromium equivalent equations. Notice the coefficient used for the chromium equivalent equation and that the lines are not linear

Post and Eberly (Ref. 22), who were concerned with austenite to pseudo-martensite transformation during cold working, reported the following equation for austenite stability:

$$Ni + 0.5Mn + 35C = \frac{(Cr + 1.5Mo - 20)^2}{12} + 15 \quad (3)$$

The Post-Eberly equation was used to explain austenite stability in the chromium range of 14 to 25 percent and a nickel range of 7 to 21 percent. Thus, it was shown that the Newell-Fleischmann expressional form was satisfactory in the prediction of austenite stability relative to both delta ferrite and martensite.

The concept of equivalence started to take a more established form when Campbell and Thomas (Ref. 15) reported that 25 chromium 20 nickel weld metal microstructure and mechanical properties could be correlated to small additions of molybdenum and columbium by using a chromium equivalent expression, which was written as chromium equivalent = Cr + 1.5Mo + 2Cb. Binder, Brown and Franks (Ref. 24) reported austenite stability relative to delta ferrite is given by:

$$Ni + 30C + 26N = 1.3Cr - 11.1 \quad (4)$$

Thomas (Ref. 19) suggested the following more inclusive linear equation for predicting the austenite stability boundary relative to delta ferrite formation:

$$Ni + 0.5Mn + 30C = 1.1\,(Cr + Mo + 1.5Si + 0.5Cb) - 8.2 \quad (5)$$

These were the first steps towards the linearization of the final Schaeffler and DeLong diagrams.

Schaeffler (Ref. 17), using the above concepts for microstructural correlation and an extensive experimental effort, made a diagram which had compositional variables on the axes and ranges for the specific weld metal microstructural phases plotted in the diagram. The coordinates of the diagram were given as nickel-equivalent and chromium-equivalent, on the vertical and horizontal axes, respectively. This choice of axes allows correlation of the effects of the "austenite formers" (Ni, Mn, C, etc.) and the "ferrite formers" (Cr, Mo, etc.) on the final microstructure. One of the original Schaeffler diagrams is seen in Fig. 2.

The original Schaeffler nickel equivalent equation, which has compositions given in weight percent, is described (Ref. 17) as follows:

$$Ni(eq) = Ni + 0.5Mn + 30C \quad (6)$$

This equation is consistent with the earlier finding of Newell and Fleischmann (Ref. 8). This empirical expression indicates that, in comparison to manganese, nickel

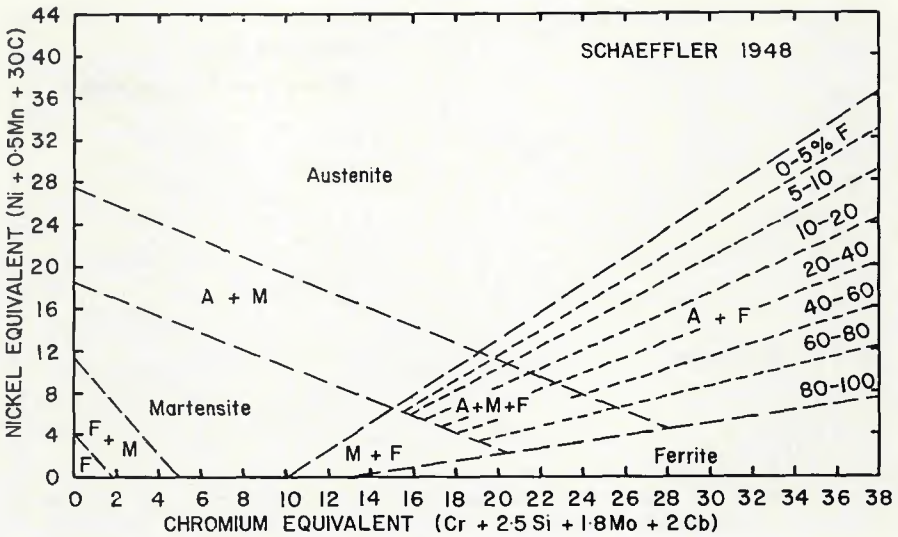

Fig. 3 – The Schaeffler diagram of 1948 gives a more quantitative description of the ferrite content and the lines were presented as linear

is twice as effective as an austenite stabilizer. Notice the extremely strong austenite stabilizing influence of carbon. The original Schaeffler chromium equivalent equation is given (Ref. 17) by:

$$Cr(eq) = Cr + 1.8Mo + 2.5Si + 2Cb \quad (7)$$

Notice on the original Schaeffler diagram, as seen in Fig. 2, that the phase boundary lines have curvature. This curvature, which suggests elemental synergistic effects, implies that these equivalence equations should have had cross terms if the lines on the diagram were to be linear. The experimentally determined curved boundary lines between fully austenite weld metal and the austenite-plus-ferrite region were reported by Schaeffler (Ref. 17) to be expressed mathematically by the equation

$$Ni_{eq} = \frac{(Cr_{eq} - 16)^2}{12} + 12 \quad (8)$$

It is interesting that the quadratic nature of the austenite stability showed up as late as 1969, when Griffith and Wright (Ref. 169) reported the following equation:

$$Ni + 0.5Mn + Cu + 35C + 27N = 1/12\,(Cr + 1.5Mo - 20)^2 + 15 \quad (9)$$

Notice the similarity of this equation with the expressions of Newell and Fleischmann (Ref. 8), Feild, Bloom and Linnert (Ref. 10), and Post and Eberly (Ref. 22), which were described above. It must be remembered in reviewing the work of various investigators that the heat input (and thus cooling rate) influences the nature of the solidified microstructure and will also cause shifts in these curves.

A Schaeffler diagram, nearly as we now know it, can be seen in Fig. 3. This diagram was introduced (Ref. 18) in 1948. It increased the ability to quantitatively predict weld metal microstructure, especially in the two phase region of austenite and delta ferrite. Also notice the synergistic influence of chromium on the austenitic stability of nickel. It takes approximately 30 weight percent nickel to stabilize austenite with no chromium, but only 12 weight percent nickel with 19 weight percent chromium. This diagram has a chromium equivalent as suggested in equation 7.

Schaeffler (Ref. 17) also demonstrated on his original diagram a method to graphically predict weld metal microstructure as a function of the amount of base plate dilution. In 1949, Schaeffler (Ref. 1) reported a modified diagram as seen in Fig. 4. It is this diagram that is used today. The major modification is with the chromium equivalent expression, which was changed to be

$$\text{Chromium Equivalent} = Cr + Mo + 1.5Si + 0.5Cb \quad (10)$$

Seferian (Ref. 27) developed an expression to calculate the amount of delta ferrite from these nickel and chromium equivalent expressions. This expression is given as:

$$\text{delta ferrite} = 3[Cr_{eq} - 0.93Ni_{eq} - 6.7] \quad (11)$$

where the nickel and chromium equivalents are calculated using the Schaeffler equations.

Two other similar diagrams have been reported. Schneider (Ref. 25) developed in 1960 a diagram for the prediction of cast microstructure, as seen in Fig. 5. This diagram introduced cobalt and vanadium to the nickel and chromium equivalent, respectively. Kakhovskii, et al. (Ref. 26), reported the diagram illustrated in Fig. 6 for

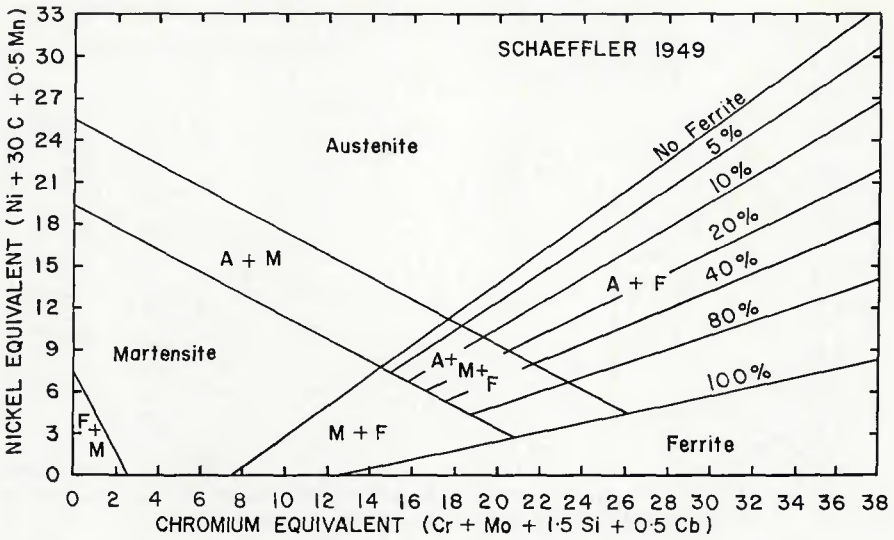

Fig. 4 — The Schaeffler diagram of 1949, the diagram which is commonly used to predict ferritic-austenitic dissimilar weld metal microstructure, had coefficient changes in the chromium equivalent expression when compared to the Schaeffler diagram of 1948

weld metal, which also quantifies the alloying influence of vanadium and titanium.

The Schaeffler diagram (Fig. 5) is divided into regions based on the transformation behavior of austenite. Liquid to austenite and austenite to martensite transformations are on the left of the diagram, while liquid to ferrite transformations are on the right. The mechanism of this martensite (diffusionless) transformation is understandably different from those of the nucleation-and-growth of ferrite from liquid.

DeLong and Reid (Ref. 28) investigated the portion of the original Schaeffler diagram which is important to the compositional range of austenitic stainless steel and constructed a diagram. This diagram, seen in Fig. 7, has been very instrumental in advancing the utilization of stainless steel, in that it allowed for quantitative and reproducible prediction of the amount of delta ferrite. It has been accepted as practice to expect that austenitic stainless steels should have a single phase austenitic structure after rolling and annealing, but 3-8% delta ferrite is expected in the austenitic weld metal to reduce the susceptibility of hot cracking in austenitic stainless steel welds. DeLong and Reid introduced a modification to the nickel equivalent expression by adding the influence of nitrogen. The nickel equivalent equation, then, is given as follows:

$$Ni_{eq} = Ni + 0.5Mn + 30C + 30N \quad (12)$$

Notice that the nitrogen was found to have the same influence of austenitic stability as carbon. Long and DeLong (Ref. 29) made further changes to this diagram by altering the lines after an extensive experimental and analytical analysis to improve its ability to predict delta ferrite. This diagram is given in Fig. 8. They also made some evaluation of the experimental and statistical error in its use. They found that with filler metals of types 308, 308L and 347 stainless steels the Schaeffler and DeLong diagrams are essentially equal, except at high nitrogen levels, in their ability to predict stainless steel weld metal microstructure. The Schaeffler diagram, as reported in Fig. 9, was found to underestimate the ferrite content for the filler materials of types 316, 316L and 309 stainless steels. The revised DeLong diagram was determined to be an improvement for these higher alloyed stainless steels. Long and DeLong (Ref. 29) reported that their diagram is fairly insensitive to typical heat input variations found in arc welding.

Tables 1 and 2 list the reported coefficients for elements in the nickel and chromium equivalent equations for predicting delta ferrite. Much of the apparent variation is due to the broad range of alloys from which these coefficients were generated.

Szumachowski and Kotecki (Ref. 30) have recently found better agreement between calculated and measured ferrite numbers for an extended manganese range, up to 12.5 weight percent, by using a modified nickel equivalent equation. The original DeLong nickel equivalent expression, which has been found to be very useful for manganese contents common to the 300 series stainless steel, was found to seriously underestimate the

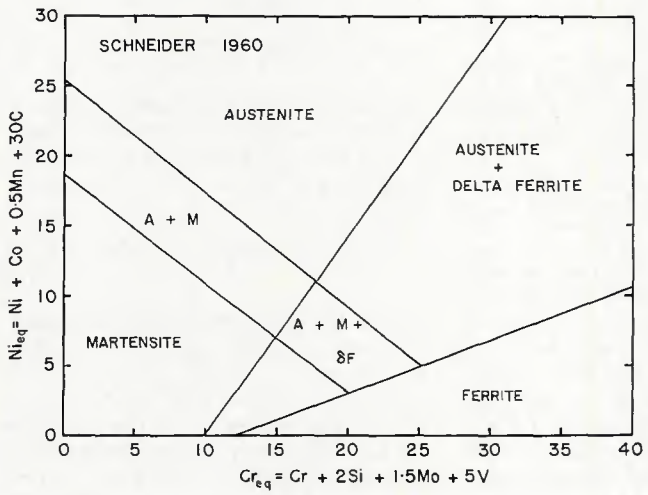

Fig. 5 — The Schneider diagram, which was developed for cast materials, reports the influence of cobalt and vanadium on the nickel and chromium equivalent expressions

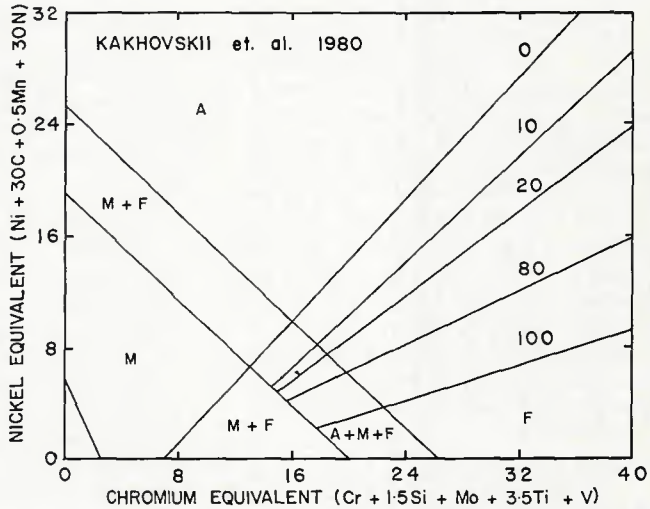

Fig. 6 — The Kakhovskii diagram, which was developed for weld metal, reports the influence of titanium and vanadium on weld metal microstructure. Notice the discrepancy in the coefficient for vanadium when compared to the Schneider diagram

ferrite number of weld metal above 2.5 weight percent manganese. They replaced the 0.5Mn term by a small constant. The modified nickel equivalent was reported to be

$$Ni_{eq} = Ni + 30(C + N) - 0.35 \quad (13)$$

The coefficient for manganese in the nickel equivalent equation has been in question ever since the first Schaeffler diagram (Ref. 19). It has been reported, based on armor welding during World War II, that above 4 percent manganese there is some question about the use of a coefficient of ½. Hull (Ref. 31) investigated stainless steel castings with high manganese contents and reported the diagram that is seen in Fig. 10. Figure 10 indicates the austenite to delta ferrite boundary. The nickel equivalent, which also has terms for cobalt, copper and nitrogen, has two terms for manganese: one linear term with a coefficient of 0.11 and a square term with a coefficient of 0.0086.

The molybdenum coefficient has been reported to have a value between one and two, as seen in Table 2. Kotecki (Ref. 32) reexamined the effect of molybdenum on the ferrite number and the chromium equivalent expression. The DeLong chromium equivalent expression, as seen in equation 10, suggests that molybdenum additions have the same influence in promoting ferrite as do chromium additions. Kotecki found that the WRC-DeLong diagram (Fig. 8) overestimated the ferrite number on the weld metal and this overestimation can be corrected by using a molybdenum coefficient of 0.7. In a similar investigation, Novozhilov, et al. (Ref. 33), found that the value should be 1.5.

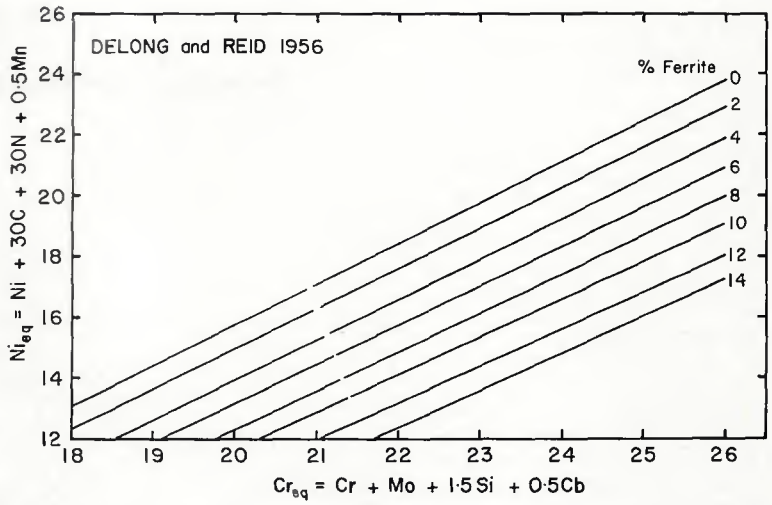

Fig. 7 — The DeLong and Reid diagram of 1956, which was designed for the range of composition for stainless steel, introduces the influence of nitrogen to the determination of the amount of delta ferrite in stainless steel weld metal

Schoefer (Refs. 34-36) developed a diagram, as seen in Fig. 11, for predicting the amount of delta ferrite in cast Fe-Cr-Ni alloys. This diagram has the coordinates of the chromium equivalent to nickel equivalent ratio and ferrite number. Schoefer modified the nickel and chromium equivalents for use with his diagram and they are given as follows:

$$Cr_{eq} = Cr + 1.5Si + Mo + Cb - 4.99 \quad (14)$$

and

$$Ni_{eq} = Ni + 30C + 0.5Mn + 26(N - 0.02) + 2.77 \quad (15)$$

The Schaeffler and Schoefer diagrams would be expected to predict different results since the solidification and cooling rates are very different.

Potak and Sagalevich (Ref. 37) proposed a new form for constitutional diagram (Fig. 12) for the prediction of stainless steel cast and weld metal microstructure. This diagram has a horizontal axis for ferrite stability expression called the ferrite formation equivalents, Cr^F_{eq}, and a vertical axis for martensite stability called the martensite formation chromium equivalent, Cr^M_{eq}. These chromium equivalent expressions, which are given in Fig. 12, are very comprehensive in considering potential alloy additions. The elemental coefficients are different, depending on whether they are relating to a martensitic or liquid to ferrite transformation. This diagram is reported to allow for better ability to predict in the region of martensite-ferrite-austenite triplex weld metal microstructure. The coefficients K_M and K_F for carbon and nitrogen vary from 25 to 65, depending on the carbon and nitrogen concentrations and the type of transformation being described. A K_M and K_F diagram is incorporated into Fig. 12 to allow for the selection of these coefficients.

The concept of the Potak and Sagalevich diagram construction (Ref. 37) has also been extended by Barmin and Korolev (Ref. 38) to the prediction of the amounts of martensite, austenite and primary Laves phases. Figure 13 illustrates a diagram which has vertical axis parameter given by:

$$\beta_\gamma = 18 - 1.5Ni + 0.1Co - 0.7Mo - 0.5Ti - 0.2Si \quad (16)$$

where β_γ represents austenite stability expression. When $\beta_\gamma = 0$, this equation describes the phase boundary between martensite and martensite-austenite at

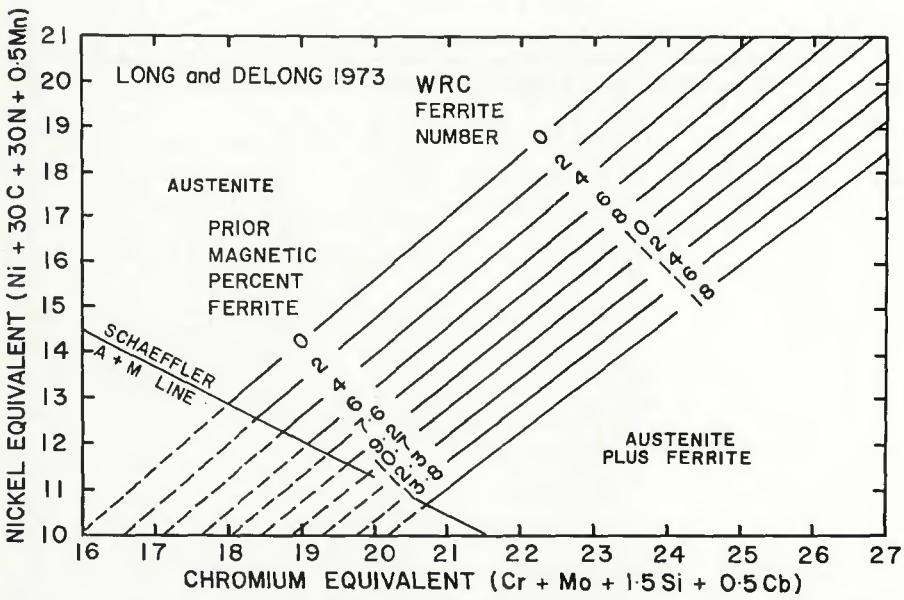

Fig. 8 — The Long and DeLong diagram of 1973 improved the accuracy of the earlier DeLong and Reid diagram and also introduced the scale for ferrite number

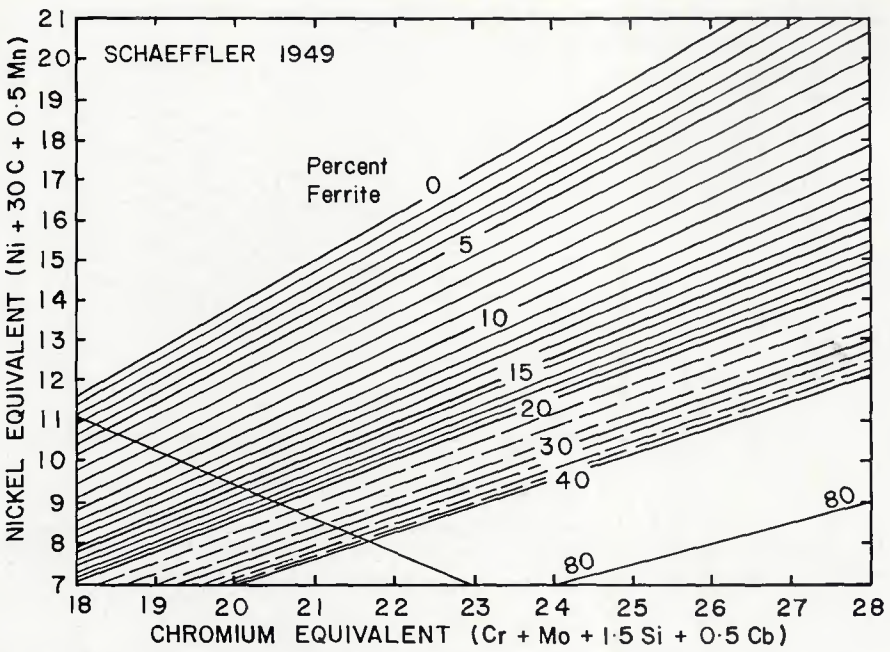

Fig. 9—The Schaeffler diagram of 1949 with a refined percent ferrite scale

room temperature. The horizontal axis is described by a parameter, β_ϵ, where

$$\beta_\epsilon = 2.5 - 0.01Ni - 0.06Co - 0.12Mo - 0.50Ti - 1.00Si \quad (17)$$

where β_ϵ relates the influence of alloy composition to promote Laves phase formation.

Role of Delta Ferrite

The hot cracking susceptibility of austenitic stainless steels is reduced with a duplex microstructure (Refs. 39-68). Investigators contend that three to eight volume percent delta ferrite is required to reduce hot cracking susceptibility. However, ferrite is not a sufficient condition to prevent hot cracking. Recent investigations have shown that a primary ferrite solidification mode is also necessary (Refs. 69-104). To ensure primary ferrite solidification, alloy composition must lie on the effective chromium-rich side of the liquidus projection line on the Fe-Cr-Ni phase diagram shown in Fig. 14.

The liquidus line starts on the iron-nickel as a peritectic three phase reaction. The peritectic behavior will occur until the liquidus line crosses the austenite solidus line, which occurs at approximately 8 weight percent chromium and 5.5 weight percent nickel. After crossing the austenite solidus, the liquidus stays between the ferrite and austenite solidus lines, which represents the eutectic type reaction that is illustrated in the isopleth shown in Fig. 15. Fredriksson (Ref. 105) has investigated the solidification behavior in iron-base alloys in the region where there is a transition behavior from peritectic to eutectic reaction behavior.

Suutala, et al. (Refs. 73, 74), determined the liquidus projection line as a function of modified nickel and chromium equivalent expressions, as seen in Fig. 16. He clearly distinguishes the regions of primary ferrite and primary austenite. Suutala indicates the location of the liquidus line on the DeLong diagram in Fig. 17. It is clear from Fig. 17 that not all ferrite is primary ferrite and that using ferrite content as a measure of hot cracking susceptibility must be done with discretion. Suutala (Ref. 74), Vitek and David (Ref. 102), and Lippold (Ref. 167) have illustrated that the boundary between primary austenite and primary ferrite solidification is not just a function of weld metal composition, but is a function of the growth rate when the welding process promotes growth rates greater than 10 mm/s (0.39 in./s).

Delta ferrite amount, morphology and distribution required to produce optimal weld strength were determined to be service temperature dependent. At low service temperatures, delta ferrite has a ductile to brittle transition temperature (Refs. 106, 107). Therefore, a weld metal microstructure containing a low ferrite content with a noncontinuous network is desired to limit brittle crack propagation. Less than eight volume percent delta ferrite is required to insure a noncontinuous network. For each type of austenitic stainless steel, there is a specific volume-percent of delta ferrite which yields optimum strength.

At high temperature, delta ferrite transforms to sigma phase, which is brittle (Refs. 108–110), thus, also requiring control of the ferrite content. For type 316 stainless steel, five volume percent delta ferrite provides a noncontinuous network and optimum high temperature creep strength (Ref. 110).

The Fe-Cr-Ni-N Weld Metal System

Small amounts of nitrogen in austenitic stainless steels have been known to alter microstructure-sensitive properties and are probably the greatest source of error in using the diagrams. Early investigators studied nitrogen as a solid solution strengthener and as a potential substitute for a certain amount of nickel in austenitic stainless steel (Refs. 111–119). It was determined that nitrogen acted as a solid solution strengthener similar to carbon; however, the nitrogen strengthening

Table 1—Nickel Equivalents for Delta Ferrite Prediction

Ni	Mn	Mn^2	C	N	Cu	Co	Investigators	Ref.
1.0			17.0	11.0			Avery	166
1.0	0.5		30.0				Feild, Bloom and Linnert	10
1.0	0.5		30.0				Henry, Claussen and Linnert	164
1.0	0.5		30.0				Schaeffler	1
1.0	0.5		30.0	30.0	0.3		Ferree	165
1.0	0.5		30.0	30.0			DeLong and Reid	28
1.0			30.0	20.0			Guiraldenq	64
1.0	0.5		27.0	37.0	0.5	0.4	Potak and Sagalevich	37
1.0	0.5		30.0	10-25	0.6		Castro and de Cadenet	58
1.0	0.5		30.0			1.0	Schneider	25
1.0	0.11	0.82	24.5	18.4	0.44	0.41	Hull	31
1.0	0.5		30.0	13.6			Okagawa, et al.	124
1.0	0.31		22.0	14.2	1.0		Suutala	126
1.0	0.5		30.0	30.0			Kakhovskii, et al.	26
1.0	0.5		30.0	8-45.0			Norozhilov, et al.	33
1.0	0[a]		30.0	30.0			Kotecki	30

[a]Mn functionality is replaced by a constant of 0.35.

effect was found to be temperature dependent (Refs. 120-122).

Small nitrogen variations alter delta ferrite content in weld metal microstructures (Refs. 29, 33, 123-127). Investigators have empirically described the austenitizing effect of specific alloying elements relative to nickel (Ref. 17). A variety of nitrogen coefficients have been determined (Refs. 28, 29, 33, 74, 124, 125, 128) for these nickel equivalent expressions and are listed in Table 1. The recent values of 13 to 14 for the 18Cr-8Ni stainless steel weld metal are probably better estimates than the earlier reported value of 30. The weld metal nitrogen content of austenitic stainless steel was found to be a function of the welding variables (Refs. 129, 130).

The weld metal concentration has been measured as a function of the partial pressure of nitrogen in the argon shielding gas. The weld metal nitrogen content has an apparent parabolic relationship (Refs. 77, 93, 131). Arata (Ref. 131) reported data which suggests that the base metal nitrogen content is in a form which does not take part in the gas solubility reaction during welding. The observation develops from the fact that the weld metal nitrogen content is the same as the original base metal when the pure argon shielding gas is used (Ref. 131). The total weld metal nitrogen content is the sum of the residual nitrogen content of the melted base metal and the nitrogen picked up from the shielding gas-metal interaction (Ref. 124).

Since the base metal nitrogen content apparently does not enter the gas-metal equilibrium during welding, Okagawa, et al. (Ref. 124), normalized the weld metal nitrogen concentration data by subtracting the base metal nitrogen concentration from the measured weld metal nitrogen concentration. When the normalized nitrogen concentrations squared is plotted as a function of nitrogen shielding gas partial pressure from the data of a number of investigators (Refs. 77, 117, 124), all the data correlated well, suggesting that most investigators observed the same gas-metal reaction.

Soluble nitrogen was found to have a major influence on the weld metal microstructure; in particular, the quantity and distribution of delta ferrite. The base metal nitrogen is apparently in a form which does not influence the weld metal solidification behavior. Figure 18 includes the ferrite content measurements of Okagawa, et al. (Ref. 124), Cieslak, et al. (Ref. 77), and Espy (Ref. 117) as a function of normalized weld metal nitrogen content. The agreement suggests that the ferrite content is not a function of the total weld metal nitrogen, but only a function of that part which is in solid solution. These findings again suggest that the base metal nitrogen is in a form which does not influence weld metal solidification behavior during the short period of the welding cycle. The large variation in nitrogen coefficient for the nickel equivalent expression is probably associated with correlating both the nonsoluble and soluble nitrogen contents to the weld metal microstructure.

Molinder (Ref. 132) has reported that weld metal microstructures of titanium

Table 2—Chromium Equivalents for Delta Ferrite Prediction

Cr	Si	Cb	Mo	Ti	Al	V	W	Ta	Mn	Investigators	Ref.
1.0	1.6	2.8								Avery	166
1.0			2.0							Feild, Bloom and Linnert	10
1.0		2.0	1.5							Campbell and Thomas	15
1.0	2.5	2.0	1.8							Schaeffler	17
1.0	1.0	2.0	2.0	5.0						Henry, Claussen and Linnert	164
1.0	1.5	0.5	1.0							Schaeffler	1
1.0	1.5									Ferree	165
1.0				3.5						Runov	66
1.0	1.5	0.5	1.0							DeLong and Reid	28
1.0	1.5		2.0	4.0	3.0				0.45	Guiraldenq	64
1.0	2.0	0.9		4.0	4.0	1.5	0.5			Potak and Sagalevich	37
1.0	0.48	0.14	1.21	2.2	2.48	2.27		0.21		Hull	31
1.0	1.5	1.0	1.0							Schoefer	36
1.0	1.5	0.5	1.0	2-5			0.5			Castro and de Cadenet	58
1.0	2.0		1.5			5.0				Schneider	25
1.0	1.5		1.0	3.5		1.0				Kakhovskii, et al.	26
1.0	1.5	2.0	1.37	3.0						Suutala	126
1.0			1.5							Norozhilov, et al.	33
1.0	1.5	0.5	0.7							Kotecki	32

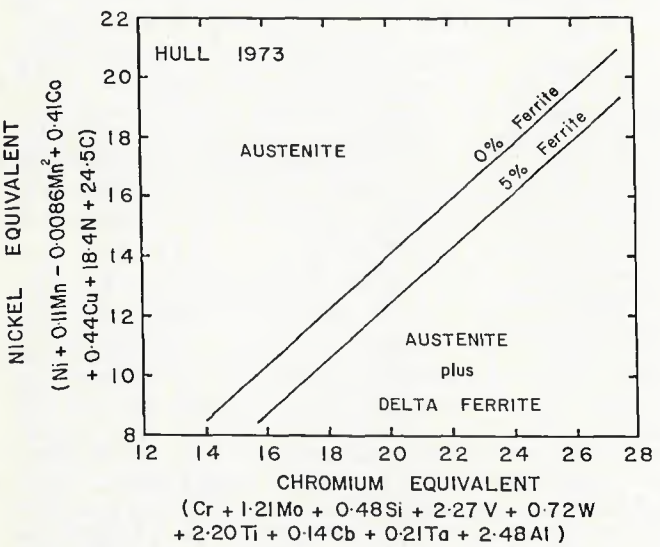

Fig. 10—The Hull diagram determines the austenite stability boundary relative to ferrite using coefficients which consider the influence of fifteen different alloy additions

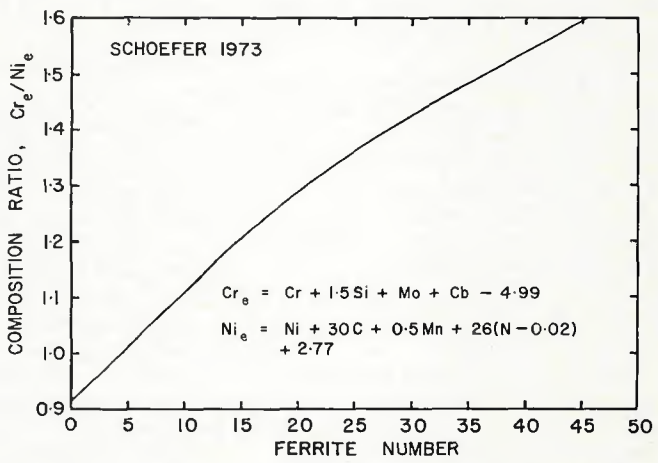

Fig. 11—Schoefer diagram plots the ratio of the chromium equivalent to nickel equivalent as a function of ferrite number. This diagram is used to predict ferrite content in cast metal

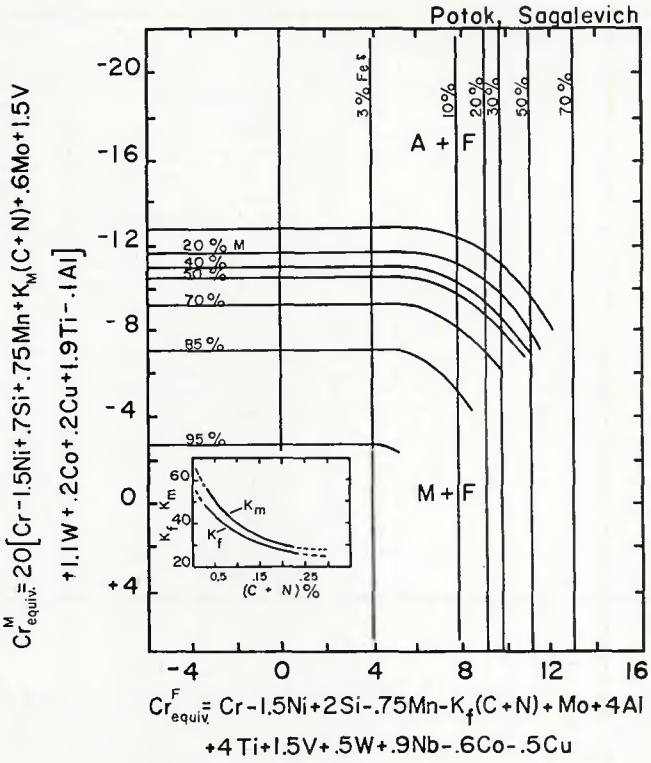

Fig. 12—Potak and Sagalevich diagram for the prediction of stainless steel cast and weld metal microstructure

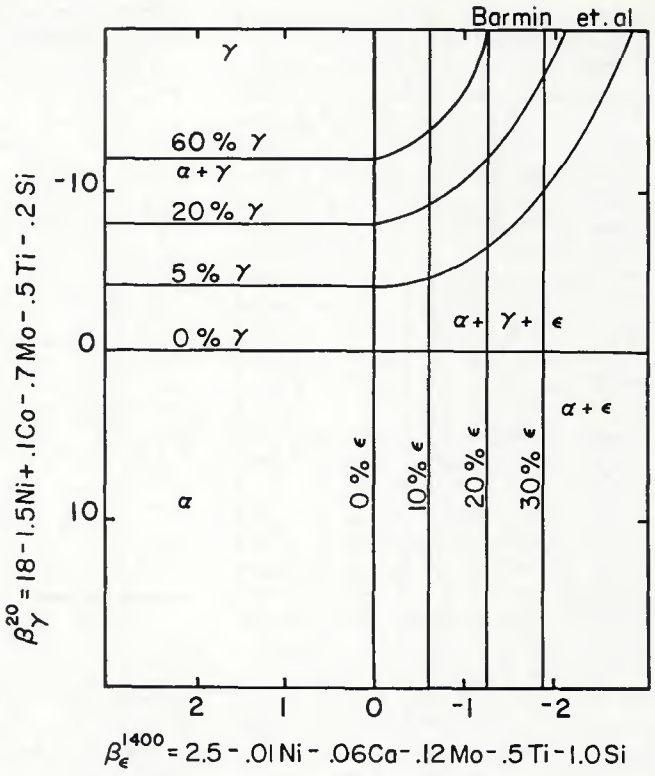

Fig. 13—Barmin and Korolev diagram for the prediction of the amounts of martensite, austenite and primary Laves phases

stabilized grades of austenitic stainless steel cannot be accurately predicted by the DeLong diagram. The influence of carbon and nitrogen to promote the austenite phase in these stabilized stainless steels is reduced by the removal of these elements from solution by titanium carbide and nitride formation. The ferrite forming ability should be related to the residual uncombined titanium and not the total titanium content. For titanium stabilized weld metal, Molinder reported that this grade can be considered as unstabilized steel with C + N greater than 0.030 weight percent.

Pryce and Andrews (Ref. 133) have introduced expressions to calculate effective titanium and columbium contents to be used to predict solid solution stability. These equations subtract the titanium and columbium contents which are assumed to be tied up as precipitates. These equations are given as:

$$Ti_{eff} = Ti - 4\,[(C - 0.03) + N] \quad (18)$$
$$Cb_{eff} = Cb - 8\,[(C - 0.03) + N] \quad (19)$$

It is not surprising that there is a large discrepancy in the nitrogen coefficient, considering it is very difficult to determine the most significant nitrogen content which is the nitrogen that is in solid solution.

One method to account for the proper content of alloying addition which is to be used for the prediction of phase stability is by the PHACOMP analysis (Refs. 133, 134). PHACOMP analysis has been used to predict whether a superalloy will produce sigma phase. This analytical approach determines the amount of the alloy contents that are associated with precipitates or second phases and adjusts the alloy contents to obtain the content of the solid solution. The PHACOMP uses the adjusted composition to make microstructural prediction.

The Fe-Mn-Ni-Cr Austenitic Weld Metal

The Fe-Mn-Ni system was first investigated by Parravano (Ref. 136). Later, Rapatz (Ref. 137), Spraragen and Claussen (Ref. 138), Avery and Chapin (Ref. 139), Avery (Ref. 140), Danhier (Ref. 141), DeLong (Ref. 142), and DeLong and Reid (Ref. 143) made important contributions for welding applications. Hochmann (Ref. 144) and Tavadze and Grikurov (Ref. 145) have reported on the complex role of manganese additions in austenitic stainless steels. The phase stability of Fe-Mn-Ni-Cr austenitic weld metal was recently evaluated by Self, et al. (Ref. 146), over a composition range greater than that considered by the original Schaeffler construction. The weld metal microstructures for compositions less than 18 weight percent chromium consist of austenite and martensite in volume fractions which range from fully austenitic to fully martensitic weld metal. Self, Olson and Matlock (Ref. 146) were interested in the ability of the Schaeffler nickel and chromium equivalent expression to predict the martensitic transformation in high alloy weld metal.

The effect of alloying upon the M_s temperature in low-chromium alloy steels has been previously reported (Refs. 147–149), though not specifically for weld metal. The Andrews equation, with alloy contents in weight percent,

$$M_s = 539 - 423C - 30.4Mn - 17.7Ni - 12.1Cr - 7.5Mo \quad (20)$$

has been found to predict the approximately 100 percent-austenite phase boundary in an Fe-Mn-Ni weld metal system with chromium contents of less than five weight percent. Thus, by assuming that the martensite start temperature, M_s, of interest is 20°C (68°F), equation 20 reduces to

$$17.07 - 13.9C - Mn - 0.58Ni - 0.40Cr - 0.25Mo = 0 \quad (21)$$

Self, et al. (Ref. 146), found that equation 21 describes well the martensite start temperature for their Fe-Mn-Ni-Cr weld with chromium contents less than one weight percent. It should be noted that this expression (equation 21) is not consistent with the expressions used by Schaeffler since it is apparent that manganese was found twice as effective at austenitizing than nickel, just opposite of the Schaeffler suggestion. With Fe-Mn-

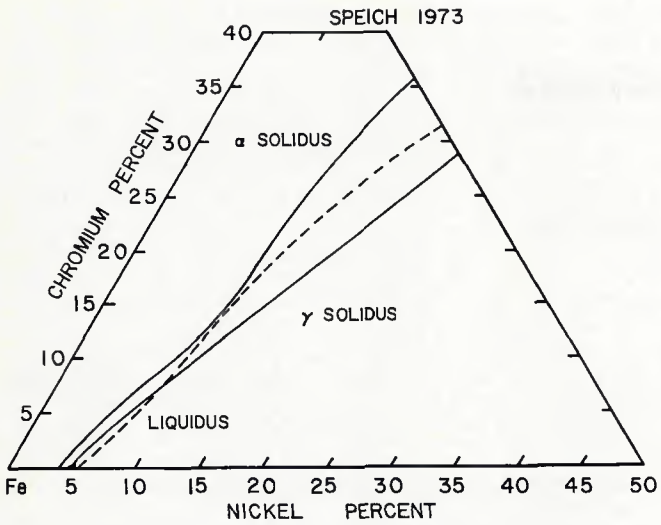

Fig. 14 — The liquidus, ferrite solidus and austenite solidus projection lines plotted on the Iron-Chromium-Nickel Ternary diagram

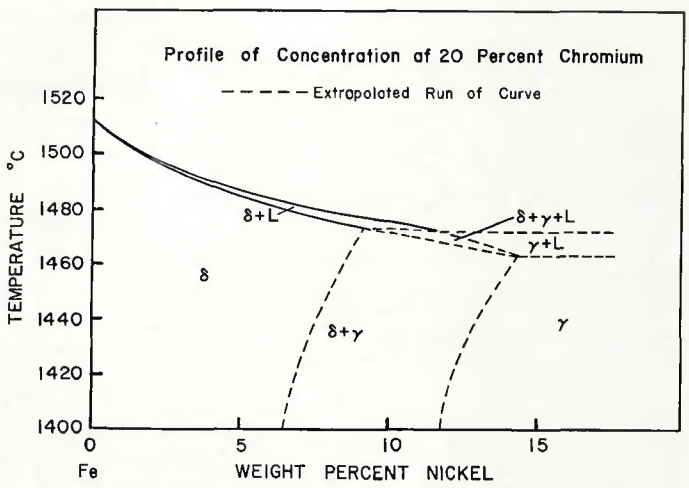

Fig. 15 — The Chromium-Nickel equivalent-20% chromium Isopleth section

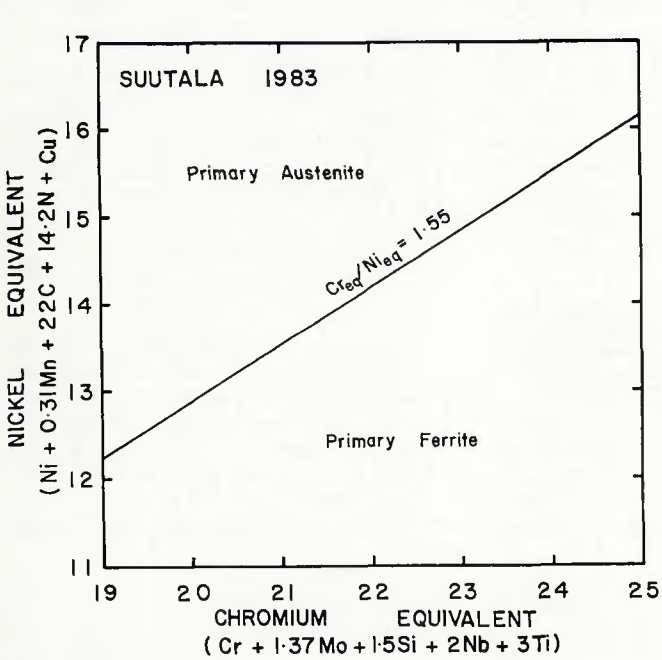

Fig. 16 — The Suutala diagram indicates the liquidus projection line as a function of nickel and chromium equivalents

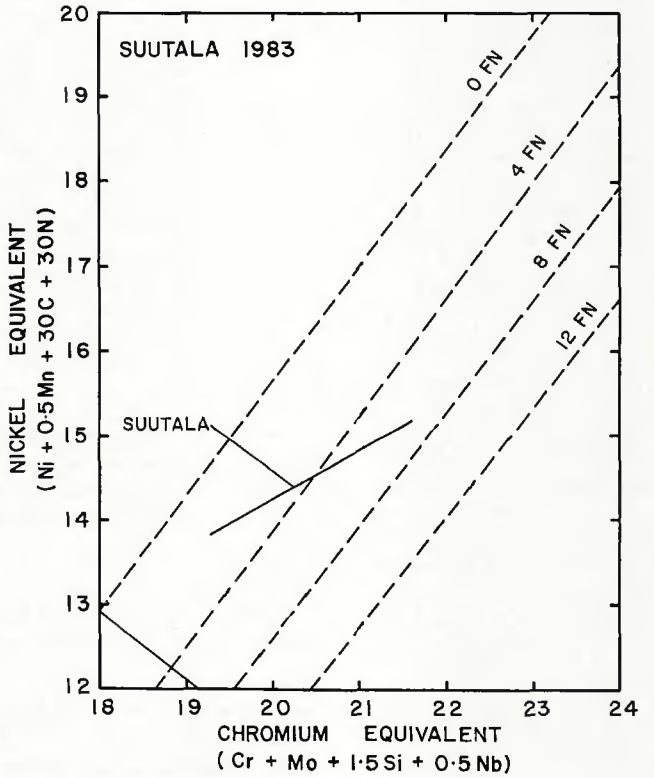

Fig. 17 — The liquidus projection line as calculated by Suutala plotted on Long-DeLong diagram

Ni-Cr weld metal with chromium content in the range of nine weight percent, significant departure was found for the 100 percent-austenite boundary predicted from an evaluation of the Andrews equation. For this chromium level, manganese and nickel exhibit approximately equal efficiencies in stabilizing austenite. At nine percent chromium the manganese and nickel relationship to austenite stability is also not correctly described by 0.5Mn:1Ni relation suggested by Schaeffler (Ref. 1) at this chromium concentration.

However, Eichlemann and Hull (Ref. 150) have shown that at even higher chromium levels (greater than 16%) the Mn:Ni coefficient ratio does approach the value suggested by Schaeffler. Using their martensite start temperature of 20°C (68°F), the austenite-martensite line is described by

$$38.59 - Mn - 50.1(C + N) - 1.83Ni - 1.25Cr - 0.83Si = 0 \quad (22)$$

It is apparent that the effect of nickel to stabilize the austenite phase is being enhanced and/or the effect of manganese is being retarded by the addition of chromium. The former is indicated, since the synergistic effect of chromium and nickel on austenite stabilization in stainless steels has already been reported (Ref. 151). A best-fit general criteria for the range of 0-16 weight percent chromium to achieve fully austenite weld metal has been reported by Self, Olson and Matlock (Ref. 146) to be:

$$Mn + [0.0833(Cr) + 0.5]Ni + 0.0742(Cr)^2 - 1.2Cr > 14.00 \quad (23)$$

Self, Olson and Matlock (Ref. 146) simplified their austenite stability criteria, rearranged variables and replotted their room temperature martensite start com-

positions in Fig. 19. Both original Schaeffler data and their own were plotted to test their modified nickel equivalent expression. Apparently, the original nickel equivalent expressions cannot describe both regions of the Schaeffler diagram accurately (the solidification formation of delta ferrite and the athermal martensitic transformation).

It should be noted from equation 23 that there is an interaction between chromium and nickel, and a self-interaction of chromium, as indicated by the $(Cr)^2$ term. The 0.083(Cr)(Ni) term expresses the synergistic stabilization of austenite by nickel and chromium, while the $(Cr)^2$ term is an expression of non-ideal solution behavior of chromium, which becomes appreciable when chromium atoms become nearest-neighbors for compositions greater than six percent chromium. It is also interesting that the $(Cr)^2$ term was in early equations of Newell and Fleischmann (Ref. 8), Feild, Bloom and Linnert (Ref. 14), and Post and Eberly (Ref. 22).

Self, Olson and Edwards (Ref. 152), using a statistical regression analysis of the data from 16 different investigations, obtained an expression for martensite start temperature as a function of alloy composition. This equation is given as:

$$M_s = 526 - 12.5Cr - 17.4Ni - 29.7Mn - 31.7Si - 354C - 20.8Mo - 1.34(CrNi) + 22.4(Cr + Mo)C \quad (24)$$

This equation does incorporate the switch in the relative austenite stability experienced for manganese relative to nickel that was reported by Self, Olson and Matlock (Ref. 146) with variations in chromium content. Equation 24 also corrects for the loss in austenite promotion (Ni_{eq}) and ferrite promotion (Cr_{eq}) due to some of the carbon, chromium and molybdenum being depleted from the solid solution with the formation of second phases. Figure 20 indicates the calculated austenite-martensite start boundary line as a function of service temperature. Notice the large shift in this boundary as the temperature approaches cryogenic service.

Fe-Mn-Ni-Al Weld Metal Alloy System

The Fe-Mn-Ni-Al alloy system offers an austenitic matrix by proper alloying with manganese, nickel and aluminum additions. These alloys can have mechanical properties and corrosion resistance similar to the Fe-Cr-Ni austenitic stainless steels (Refs. 153–157). The austenitic phase stability for this weld metal alloy system has been characterized by Carpenter, Olson and Matlock (Ref. 158). Their results are illustrated in Fig. 21. Notice that both alpha and epsilon martensite can form from austenite in this alloy system. The upper right corner of the diagram achieves a microstructure very similar to type 308 stainless steel weld deposit, which is characterized by an austenitic matrix and an aluminum-rich delta ferrite phase. The nature of the stability of aluminum-rich ferrite still needs further investigation if Fe-Mn-Ni-Al weld metal is to substitute for the traditional Fe-Cr-Ni weld deposits. Notice the similarity between Fig. 21 and the original Schaeffler diagram in Fig. 4.

Thermodynamic and Kinetic Approaches in the Development of Expressions for Weld Metal Behavior Prediction

In contrast to the experimentally determined expressions discussed above, Liu, Matlock and Olson (Ref. 159) considered a fundamental approach to establish a better expressional form for these microstructural predictive equations. It is anticipated that the new expressional forms may be better suited to predict weld metal microstructure and properties over a larger compositional range. For a transformation to occur, two main conditions must be fulfilled. First is the thermodynamic desire for the transformation. Second is the kinetics of the transformation, which involves the mechanism and rate of the reaction. The martensitic transformation is most sensitive to thermodynamic desire (Refs. 148, 160), whereas the delta ferrite formation is more likely coupled to kinetic considerations.

Considering the austenite-ferrite transformation, the thermodynamic desire for transformation is given by:

$$\Delta G_{\gamma \rightarrow \alpha} = \Delta G^{\alpha}_{so1} - \Delta G^{\gamma}_{so1} \quad (25)$$

Using a modified regular solution model, this free energy change is composed of two sets of summations (Ref. 1) – the contribution of individual alloying elements and (Ref. 2) the interaction term of the alloying elements (cross product terms). If the microstructural sensitivity property, P, is directly related to the amount of transform product, Liu, et al. (Ref. 159), suggest the following expressional form should be considered:

$$P = K_{Ni}Ni + K_{Mn}Mn + K_{Si}Si + K_{Cr}Cr + K_{Cr\text{-}Mn}CrMn + K_{Cr\text{-}Si}CrSi \ldots \quad (26)$$

If the set of cross product terms is not considered, the expression suggests forms similar to the ones used for nickel and chromium equivalent equations. It becomes apparent that much of the information about alloying behavior is lost without the interaction terms, especially for the alloys with high alloying

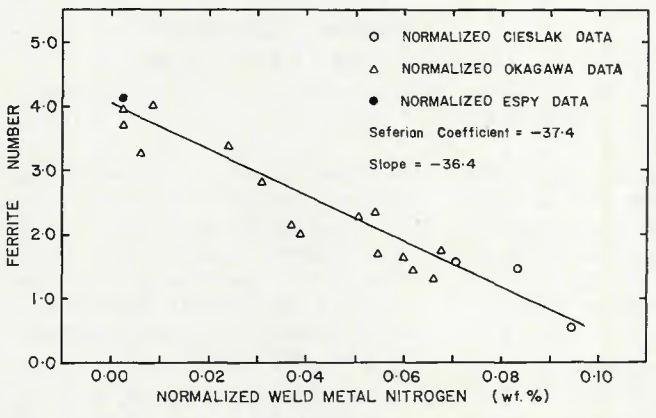

Fig. 18 – Ferrite number as a function of the normalized weld metal nitrogen content (weld metal nitrogen – base metal nitrogen). Normalized data of three investigators all lies on the same line

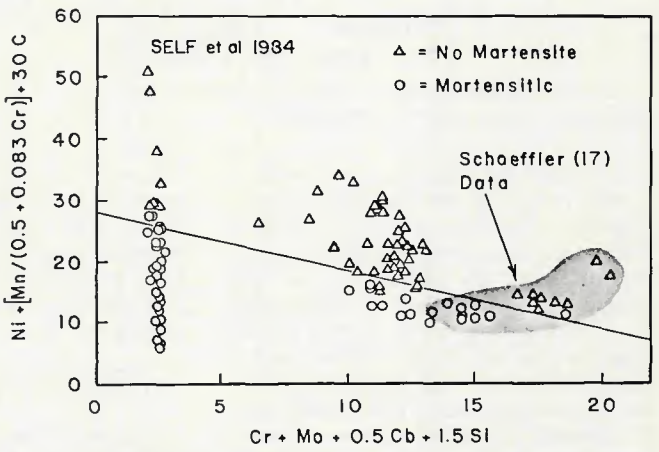

Fig. 19 – The martensite start composition for room temperature as a function of modified nickel and chromium equivalents. The Schaeffler original data was used with the results of Self, et al., to determine this line

contents. The expressional form given in equation 26 should be consistent with the evaluation of the martensitic transformation on the left side of the Schaeffler diagram.

If the kinetics is controlling the transformation, the phase stability (thermodynamic) criteria will not be sufficient for the alloy behavior prediction. It is essential to consider the transport of elements, which controls the rate of the transformation. Considering the free energy difference resulting from the difference in chemical potential for a specific element and using a modified regular solution model to describe the phases involved in the transformation, Liu, et al. (Ref. 159), suggested a general solution of the following form for the nickel and chromium equivalents:

$$Ni_{eq} = Ni\,[1 + k_{Mn}Mn + k_N N + k_c C] \quad (27)$$

$$Cr_{eq} = Cr\,[1 + k_{Si}Si + k_{Mo}Mo + k_{Nb}Nb + k_{Ti}Ti] \quad (28)$$

These nickel and chromium equivalent expressions should better fit the right side of the Schaeffler diagram where the solidification behavior controls the weld metal microstructure.

Once again, the form obtained is quite different from the nickel and chromium equivalent expressions found in the literature. Instead of only a simple summation of single element effects, a cross term (product term) should be introduced to describe the importance of the interaction between the specific element and the other alloying elements.

The Influence of Heat Input on Austenite Phase Stability in Weld Metal

Coring, which results from segregation of solidification, can be observed in weld metal microstructure. The nonhomogeneous distribution of alloying elements associated with this phenomenon is revealed by the corrugated microstructure. The nominal (average) weld metal composition of the alloying elements may be quite different from that of the composition at any given position in the weld metal. Therefore, the compositional fluctuation (above and below the nominal composition) must also be considered.

In the case of highly alloyed ferrous materials, the resulting solidification will proceed with a primary austenite or ferrite phase (depending on the composition) in the form of a dendrite or cells depleting or segregating specific alloy additions into the liquid adjacent to the solid interface. The nature and amount of sequential transformation which occurs on cooling will depend on the stability of these regions and the thermal experience. One of the ways of expressing the austenite stability for cored material, such as with weld metal, is to assume that a sinusoidal distribution function can be applied to each of the segregating elements, for example:

$$Cr = Cr_o + \Delta Cr\ Sin\left(\frac{2\pi X}{X_o}\right) \quad (29)$$

where Cr_o is the nominal composition and the ΔCr is the amplitude of the sinusoidal distribution. If some elements are segregated to the interdendritic region, then sine function is used for those elements. But if specific elements are rejected from this interdendritic region, cosine functions are to be used for them. By substituting these sinusoidal element composition equations into the nickel and chromium equivalent expressions suggested above, the variation of the austenite stability relative to a homogeneous material can be calculated by integrating the nickel or chromium equivalent equation from $X_o/2$ to X_o, where X_o is the dendritic spacing. The resulting forms should allow for the influence of cooling rate. The dendrite spacing is a function of cooling rate, which suggests that austenite stability increases for fast cooling rates and lower heat input. Self homogenization during cooling will be more complete for a smaller dendritic spacing; that is ΔMn, ΔNi, and ΔCr are smaller. For an improvement to the sinusoidal distribution model, a multiple component Scheil equation (Refs. 161, 162, 168) should be developed and considered. Such a modified Scheil equation should more adequately describe the solidification behavior of a dendrite. However, the high temperature of the welding process and the self-annealing effect suggest that the sinusoidal distribution approach is likely to give a good first order approximation of weld metal microstructure.

Conclusions

With the advent of artificial intelligence computer information retrieval systems, it is essential that our quantitative ability to

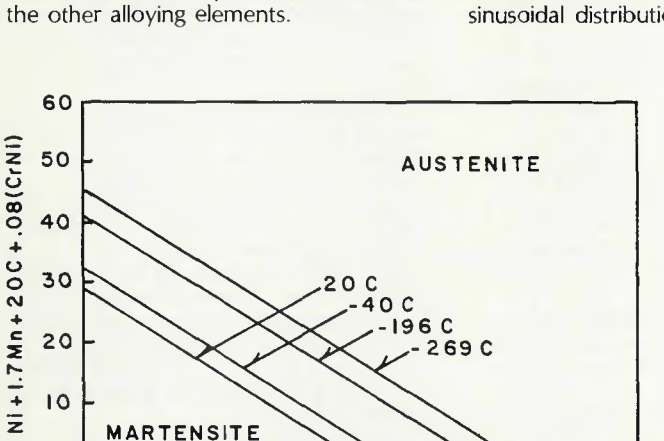

Fig. 20—The martensite start composition for various temperatures as a function of modified nickel and chromium equivalents. The (Cr+Mo)C term is only used if extensive carbide precipitation is probable

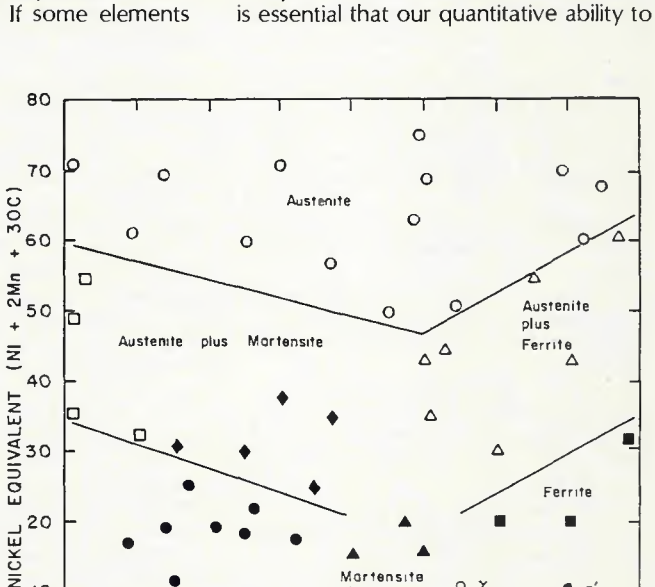

Fig. 21—An effective nickel-aluminum diagram to predict weld metal microstructure

predict austenitic weld metal microstructure and properties be carefully reviewed and analyzed. It is essential that the most comprehensive quantitative expressions for predicting microstructure as a function of composition and thermal experience be used in the software for these new computer aided design approaches for consumable selection. This paper reviewed the evolution of many of our present day diagrams for predicting weld metal microstructure associated with the use of austenitic filler materials and suggests some new analytical forms for future predictive techniques. It is anticipated that with the increase in the numerous phase transformations involved with austenitic weld deposits as the alloy additions are expanded, future predictive techniques will rely on mathematical expressions rather than diagrams to make comprehensive quantitative phase prediction of weld metal microstructure.

Acknowledgments

The author acknowledges and appreciates the research support of the Basic Energy Science Division of the United States Department of Energy. The author appreciates the information generously given by R. D. Thomas, Jr., W. T. DeLong, and D. J. Kotecki.

References

1. Schaeffler, A.L. 1949. Constitution diagram for stainless steel weld metal. *Metal Progress,* 56(11):680-680B.

2. Guillet, L. 1906. Nickel-chrome steels. *Rev. Metal,* 3:part 1, p. 332, Paris.

3. Geisen, W. 1901. The special steels in theory and practice. Iron and Steel Inst., Carnegie Scholarship Mem., 1:1.

4. Monnartz, P. 1911. The study of iron-chromium alloys with special consideration of their resistance to acids. *Metallurgie,* 8:161, Paris.

5. Maurer, E., and Strauss, B. 1912. German patents 304,126 (October) and 304,159 (December).

6. Strauss, B., and Maurer, E. 1920. Die Hochlegierten Chromnickelstahle als nichtrostende Stahle. *Kruppsche Monatshefte,* 1(8):129-146.

7. Scherer, R., Riedrich, G., and Hoch, G. 1939. Einfluss eines Gahaltes an Ferrit in austenitischen Chrom-Nickel-Stahlen auf den Kornzerfall. *Archiv. fur das Eisenhuttenwesen,* 13:52-57, July.

8. Newell, H.D., and Fleischmann, M. 1938. Hot rolled metal article and method of making same. U.S. patent No. 2,118,683.

9. Thomas, Jr., R.D. 1941. Austenitic welding in defense welding. Arcos Corporation Report, Philadelphia, Pa., September 11.

10. Feild, A.L., Bloom, F.K., and Linnert, G.E. 1943. Development of armor welding electrodes: relation of the composition of austenitic (20Cr-10Ni) electrodes to the physical and ballistic properties of armor weldments. *OSRD Report No. 1636,* July 20.

11. Schaeffler, A.L. 1944. The investigation of microstructures of single bead chromium-nickel austenitic weld deposits of SAE 4340 + V stock. MS Thesis, University of Wisconsin, June.

12. Thomas, Jr., R.D., and Ostrom, K.W. 1941. Dilution of austenitic welds by mild steels and low alloys. *Welding Journal,* 20(4):185s-188s.

13. Emerson, R.W. 1939. The effect of alloying in metallic arc welding. *Welding Journal,* 18(10):381s-392s.

14. Feild, A.L., Bloom, F.K., and Linnert, G.E. 1943. Development of armor welding electrodes: the effect of variation of chromium-nickel ratio and molybdenum content of austenitic (20Cr-10Ni) electrodes on properties of armor weldments. *OSRD Report No. 3034,* December 14.

15. Campbell, H.C., and Thomas, Jr., R.D. 1946. The effect of alloying elements on the tensile properties of 25-20 weld metal. *Welding Journal,* 25(11):760s-768s.

16. Thomas, Jr., R.D. 1946. Crack sensitivity of chromium-nickel stainless weld metal. *Metal Progress* 50(3):474-479, September.

17. Schaeffler, A.L. 1947. Selection of austenitic electrodes for welding dissimilar metals. *Welding Journal* 26(10):1-20.

18. Schaeffler A.L. 1948. Welding dissimilar metals with stainless electrodes. *Iron Age* 162:72, July 1.

19. Thomas, Jr., R.D. 1949. A constitution diagram application to stainless weld metal. *Schweizer Archiv fur Angewandte Wissenschaft und Technik,* No. 1, 3-24.

20. Rollaston, E.C., and Cottrell, A.H. 1941. The arc welding of high tensile alloy steels. *Trans. Inst. of Welding,* 4(1):9-16.

21. Hanson, D., Cottrell, A.H., Winterton, K., and Wheller, J.A. 1944. Researchers in alloy steel welding. *Welding Journal,* 23(11):573s-608s.

22. Post, C.B., and Eberly, W.S. 1947. Stability of austenite in stainless steels. *Trans. ASM,* 39:868-890.

23. Herres, S.A., and Turkalo, A.M. 1946. Welding of hardenable steels with high alloy (austenitic) electrodes. *Welding Journal,* 25(10):669s-696s.

24. Binder, W.O., Brown, C.M., and Franks, R. 1949. Resistance to sensitization of austenitic chromium-nickel steels of 0.03% max. carbon content. *Trans. ASM,* 41:1301-1346.

25. Schneider, H. 1960. Investment casting of high-hot strength 12% chrome steel. *Foundry Trade J.,* 108:562-563.

26. Kakhovskii, N.I., Lipodaev, V.N., and Fadeeva, G.V. 1980. The arc welding of stable austenitic corrosion-resisting steels and alloys. *Avt. Svarka,* No. 5, pp. 55-57.

27. Seferian, D. 1959. *Metallurgie de la Soudure,* Donod., Paris.

28. DeLong, W.T., and Reid, Jr., H.F. 1957. Properties of austenitic chromium in austenitic chromium-manganese stainless steel weld metal. *Welding Journal,* 37(1):1-8.

29. Long, C.J., and DeLong, W.T. 1973. The ferrite content of austenitic stainless steel weld metal. *Welding Journal* 52(7):281s-297s.

30. Szumachowski, E.R., and Kotecki, D.J. 1984. Effect of manganese on stainless steel weld metal ferrite. *Welding Journal* 64(5):156s-161s.

31. Hull, F.C. 1973. Delta ferrite and martensite formation in stainless steels. *Welding Journal,* 52(5):193s-203s.

32. Kotecki, D.J. 1983. Molybdenum effect on stainless steel weld metal ferrite. *IIW Document II-C-707-83.*

33. Norozhilov, N.M., et al. 1978. On the austenitizing and ferritizing effect of elements in austenitic ferrite weld metals. *Welding Prod.,* (6):12-13.

34. Schoefer, E.A. 1980. Welding of high alloy castings. Supplement 7 to the *Steel Casting Handbook.* Steel Founders' Society of America, Des Plaines, Ill.

35. Beck, F.H., Schoefer, E.A., and Flower, J.W. 1965. New cast high-strength alloy grades by structure control. ASTM Special Technique Publication No. 369.

36. Schwartzendruber, L.J., Bennet, L.H., Schoefer, E.A., DeLong, W.T., and Campbell, H.C. 1974. Mossbauer effect examination of ferrite in stainless steel welds and castings. *Welding J.,* 53(1):1s-12s.

37. Potak, M., and Sagalevich, E.A. 1972. Structural diagram for stainless steels as applied to cast metal and metal deposited during welding. *Avt. Svarka,* (5):10-13.

38. Barmin, L.N., Korolev, N.V., Grigorev, S.L., Logakina, I.S., and Manakova, N.A. 1980. The phase composition of iron-nickel-cobalt-molybdenum-titanium-silicon system deposited metal. *Avt. Svarka,* (10):22-24.

39. Thomas, Jr., R.D. 1946. Crack sensitivity of chromium-nickel stainless weld metal. *Metal Progress,* 50(3):474-479, September.

40. DeLong, W., Ostrom, G., and Szumachowski, E. 1956. Measurement and calculation of ferrite in stainless steel weld metal. *Welding Journal,* 35(11):526s-533s.

41. Hull, F.C. 1960. Effects of alloying additions on hot cracking of austenitic chromium-nickel stainless steels. *Proc. ASTM,* 60:667-690.

42. Gueussier, A., and Castro, R. 1960. Etude experimentale des criques de solidification dans les aciers influence des impuretes. *Revue de Metallurgie,* 57(2):117-134.

43. Borland, J.C., and Younger, R.N. 1960. Some aspect of cracking in welded Cr-Ni austenitic steels. *British Welding J.,* 7(1):22-60.

44. Hull, F.C. 1960. Effects of alloying additions on hot cracking of austenitic chromium-nickel stainless steels. *Proc. Amer. Soc. for Testing and Materials,* 60:607-690.

45. Castro, R. 1961. Sur la structure secondaire des aciers inoxydables austenitiques. *Mem. Sci. Rev. Met.,* 58(11):881-884.

46. Oyler, G.W., Matuszek, R.A., and Garr, C.R. 1967. Why some heats of stainless steel may not weld. *Welding Journal,* 46(12):1006-1011.

47. Hull, F.C. 1967. Effect of delta ferrite in hot cracking of stainless steel. *Welding Journal,* 46(9):399s-409s.

48. Fredriksson, H., and Van der Toorn, L.J. 1968. Hot cracking in austenitic stainless steel weld deposits. *British Welding J.,* 15:178-182.

49. Gunia, R.B., and Ratz, G.A. 1968. The measurement of delta-ferrite in austenitic stainless steels. *WRC Bulletin 132,* New York, N.Y., August.

50. Blanc, G., and Tricot, R. 1971. Solidification, segregation et homogeneisation des aciers inoxydables austenitiques contenant de la ferrite delta. *Mem. Sci. Rev. Met.,* 58(11):735-753.

51. Goodwin, G.M., Cole, N.C., and Slaughter, G.M. 1972. A study of ferrite mor-

phology in austenitic stainless steel weld metals. *Welding Journal,* 51(9):425s-429s.

52. Tamura, H. 1972. Weld cracking of austenitic stainless steel. *J. Japan Welding Society,* 41(2):127-147.

53. Fredriksson, H. 1972. The solidification sequence in an 18-8 stainless steel, investigated by directional solidification. *Met. Trans.,* 3(11):2989-2997.

54. Gooch, T.G., and Honeycombe, J. 1975. Microcracking in fully austenitic stainless steel weld metal. *Metal Construction and British Welding J.,* 7(3):146-148.

55. Takalo, T., Suutala, N., and Moisio, T. 1976. Influence of ferrite content on its morphology in some austenitic weld metals. *Met. Trans.,* 7A:1591-1592.

56. Lundin, C.D., and Spond, D.F. 1976. The nature and morphology of fissures in austenitic stainless steel weld metals. *Welding Journal,* 55(11):356s-367s.

57. Arata, J., Matsuda, F., and Katayama, S. 1976. Fundamental investigation on solidification behavior of fully austenitic and duplex microstructure and effect of ferrite on microsegregation. *Trans. of JWRI,* 5(2):35-51.

58. Castro, R.J., and deCadenet, J.J. 1974. *Welding Metallurgy of Stainless and Heat Resisting Steels,* pp. 158-174, Cambridge University Press, Cambridge, U.K.

59. Brooks, J.A., and Lambert, Jr., F.J. 1978. The effects of phosphorus, sulfur and ferrite content on weld cracking of type 309 stainless steel. *Welding Journal,* 57(5):139s-143s.

60. Blanc, G., and Tricot, R. Solidification, segregation et homogeneisation des aciers inoxydables austenitiques contenant de 51. Brooks, J.A., and Lambert, Jr., F.J. 1978. The effects of phosphorus, sulfur and ferrite content on weld cracking of type 309 stainless steel. *Welding Journal,* 57(5):139s-143s.

61. Schoefer, E. 1974. Appendix to Mossbauer effect examination of ferrite in stainless steel welds and castings. *Welding Journal,* 53(1):10s-12s.

62. Fleischman, W.L. 1954. Determination of ferrite in type 347 stainless steel weld metal deposits. *Welding Journal,* 34(9):459s-468s.

63. Binder, W.O. 1951. Interchangeability of Cb and Ta in type 347 stainless. *Metal Progress,* 59:219-227, February.

64. Guiraldenq, P. 1967. Ferrite and austenite forming tendencies on the principal alloying elements in 18Cr-10Ni stainless steel. *Revue de Metallurgie,* Memoires Scientifiques, (Part 1) 64(11):907-939.

65. DeLong, W.T. 1960. A modified phase diagram for stainless steel weld metals. *Metal Progress,* 77:98-100.

66. Runov, A.E. 1967. Selection of efficient composition of Cr-Ni austenitic steel for welded structures. *Automatic Welding,* 20(2):74-76.

67. David, S.A., Goodwin, G.M., and Braski, D.N. 1979. Solidification behavior of austenitic stainless steel filler wire. *Welding Journal,* 59(11):330s-336s.

68. Montoliu, F.C., and Pinilla, R.G. The distribution of delta ferrite in austenitic-ferritic weld beads. *Rev. Metal.,* 14(4):233-237, July-August.

69. Suutala, N., Takalo, T., and Moisio, T. 1979. Single phase solidification mode in austenitic-ferritic stainless steel welds. *Met. Trans.,* 10A:1183-1190.

70. Suutala, N., Takalo, T., and Moisio, T. 1979. The relationship between solidification and microstructure in austenitic and austenitic-ferritic stainless steel welds. *Met. Trans.,* 10A:512-514.

71. Takalo, T., Suutala, N., and Moisio, T. 1979. Austenitic solidification mode in austenitic stainless steel welds. *Met. Trans.,* 10A(8):1173-1181.

72. Suutala, N., Takalo, T., and Moisio, T. 1981. Technical note: comment on the transformation δ-γ by a massive mechanism in austenitic stainless steel. *Welding Journal,* 61:92s-93s.

73. Suutala, N., Takalo, T., and Moisio, T. 1980. Ferritic-austenitic solidification mode in austenitic stainless steel welds. *Met. Trans.,* 11A:717-725.

74. Suutala, N. 1983. Effect of solidification conditions on the solidification mode in austenitic stainless steel. *Met. Trans.,* 14A:191-197.

75. Lippold, J.C., and Savage, W.F. 1979. Solidification of austenitic stainless steel weldments-part 1, a proposed model. *Welding Journal,* 58(12):362s-374s.

76. Lippold, J.C., and Savage, W.F. 1980. Solidification of austenitic stainless steel weldments-part 2, the effect of alloy composition on ferrite morphology. *Welding Journal,* 59(2):48s-58s.

77. Cieslak, M.J., Ritter, A.M., and Savage, W.F. 1982. Solidification cracking and analytical electron microscopy of austenitic stainless steel weld metals. *Welding Journal,* 61(1):1s-8s.

78. Matsuda, F., Nakawaga, H., Uehara, T., Katayama, S., and Arata, Y. A new explanation for the role of delta ferrite improving weld solidification cracking in austenitic stainless steel. *Trans. of JWRI,* 8:105-111.

79. Matsuda, F., Nakagawa, H., Katayama, S., and Arata, Y. 1982. Weld metal cracking and improvement of 25%Cr-20%Ni (AISI 3105) fully austenitic stainless steel. *Trans. Japan Welding Soc.* 13(2):41-58.

80. Matsuda, F., Katayama, S., and Arata, Y. 1983. Solidification crack susceptibility in weld metals of fully austenitic stainless steels (Report IX)-effect of titanium on solidification crack resistance. *Trans. JWRI,* 12(2):87-92.

81. Matsuda, F., Nakagawa, H., Katayama, S., and Arata, Y. 1983. Solidification crack susceptibility in weld metals of fully austenitic stainless steels (Report VIII)-effect of nitrogen on cracking in SUS 304 weld metal. *Trans. JWRI,* 12(1):89-95.

82. Arata, Y., Matsuda, F., and Katayama, S. 1977. Solidification crack susceptibility in weld metals of fully austenitic stainless steels (Report III)-effect of ferrite, P, S, C, Si and Mn on ductility properties of solidification brittleness. *Trans. JWRI,* 6(1):105-116.

83. Matsuda, F., Nakagawa, H., Katayama, S., and Arata, Y. 1982. Improved solidification crack resistance in weld metal of 25%Cr-20%Ni (AISI 310S) fully austenitic stainless steel. *Proc. of Fourth International Symposium of Japanese Welding Society,* pp. 401-406, Osaka, Japan, November.

84. Matsuda, F., Katayama, S., and Arata, Y. Solidification crack susceptibility in weld metals of fully austenitic stainless steels (Report V)-solidification crack susceptibility and amount of phosphide and sulphide in SUS 310S weld metals. *Trans. JWRI,* 10(2):73-84.

85. Matsuda, F., Katayama, S., and Arata, Y. 1982. Solidification crack susceptibility in weld metals of fully austenitic stainless steels (Report VI)-effect of La or REM addition on solidification crack resistance. *Trans. JWRI,* 11(1):79-94.

86. Matsuda, F., Nakagawa, H., Uehara, T., Katayama, S., and Arata, Y. 1979. A new explanation for role of delta-ferrite improving weld solidification crack susceptibility in austenitic stainless steel. *Trans. JWRI* 8(1):105-112.

87. Matsuda, F., Nakagawa, H., Katayama, S., and Arata, Y. 1982. Solidification crack susceptibility in weld metals of fully austenitic stainless steels (Report VII)-effect of Mn and N on solidification crack resistance. *Trans. JWRI,* 11(2):79-85.

88. Matsunawa, A., Katayama, S., and Fujimoto, T. 1984. Solidification crack susceptibility of austenitic stainless steel weld metals. Welding Institute of CMES, *Proceeding Int. Conf. on Quality and Reliability in Welding,* China, September 6-8.

89. Brooks, J.A., Thompson, A.W., and Williams, J.C. 1983. Variations in weld ferrite content due to P and S. *Welding Journal,* 63(8):220s-225s.

90. Kujanpaa, V.P., 1984. Weld discontinuities in austenitic stainless steel sheet – effect of impurities and solidification mode. *Welding Journal,* 64(12):369s-375s.

91. Kujanpaa, V.P., Suutala, N.J., Takalo, T.K., and Moisio, T.J.I. 1980. *Metal Construction,* 12(6):282-285.

92. Kujanpaa, V., Suutala, N., Takalo, T., and Moisio, T.J.I. 1979. Correlation between solidification cracking and microstructure in austenitic and austenitic-ferritic stainless steel welds. *Welding Research International,* 9(2):55-77.

93. Lundin, C.D., Chou, C.P.D., and Sullivan, C.J. 1980. Hot cracking resistance of austenitic stainless steel weld metal. *Welding Journal,* 59(8):226s-232s.

94. Farrar, R.A., and Thomas, R.G. 1983. The microstructure and phase transformations in duplex 316L submerged arc weld metals. *Journal Mat. Sci.,* 18:3461-3474.

95. Allen, D.J. 1983. Solidification sequence in austenitic steel weld metal deposited on ferritic base material. *Metals Technology,* 10(1):24-27.

96. David, S.A., Goodwin, G.M., and Braski, D.N. 1979. Solidification behavior of austenitic stainless steel filler metals. *Welding Journal,* 58(11):330s-336s.

97. Rabensteiner, G., Tosch, J., and Schabereiter, H. 1983. Hot cracking problems in different fully austenitic weld metals. *Welding Journal,* 62(1):21s-27s.

98. Pertender, E., Rabensteiner, G., Schabereiter, H., and Tosch, J. 1979. Einfluss der Primarkristallisation und des Deltaferrits auf das Heissrissverhalten Austenitischen Cr-Ni-Schweissgutes. *Schweisstechnik,* 3:33-39.

99. Brown, E.L., Whipple, T.A., and Krauss, G. 1982. Metallography of duplex stainless steel castings. *ASM Metals Congress Publication 82091-003,* St. Louis, Missouri, October 23-28.

100. Cieslak, M.J., and Savage, W.F. 1980. Weldability and solidification phenomena of cast stainless steel. *Welding Journal,* 59(5):136s-146s.

101. Lippold, J.C. 1982. Weld cracking mechanisms in austenitic stainless steel. *Trends in Welding Research in the United States,* pp. 209-247, ASM Conference Proceedings, Metals Park, Ohio.

102. Vitek, J.M., and David, S.A. 1982. Microstructural analysis of austenitic stainless steel laser welds. *Trends in Welding Research in the United States*, pp. 243–258, ASM Conference Proceedings, Metals Park, Ohio.

103. Brooks, J.A., Williams, J.C., and Thompson, A.W. Solidification and solid state transformations of austenitic stainless steel welds. *Trends in Welding Research*, pp. 331–357, Metals Park, Ohio.

104. Zhitnikov, N.P. 1981. The hot cracking resistance of austenitic CrNi weld metal and weld zone in relation to nitrogen content. *Svar. Proiz*, (3):14–16.

105. Fredriksson, H. 1979. Transition from peritectic to eutectic reaction in iron-base alloys. *Solidification and Casting of Metals*, The Metals Society, London, pp. 131–138.

106. Read, D.T., McHenry, H.I., Steinmeyer, P.A., and Thomas, Jr., R.D. 1980. Metallurgical factors affecting the toughness of 316L SMA weldments at cryogenic temperatures. *Welding Journal*, 59(4):104s–112s.

107. Szumachowski, E.R., and Reid, H.F. 1978. Cryogenic toughness of SMA austenitic stainless steel weld metal: part 1—role of ferrite. *Welding Journal*, 57(11):325s–333s.

108. Berggren, R.G., Cole, N.C., Goodwin, G.M., Steigler, G.M., Slaughter, G.M., Gray, R.J., and King, R.T. 1978. Structure and elevated temperature properties of type 308 stainless steel weld metal with varying ferrite properties. *Welding Journal*, 57(6):167s–174s.

109. Spruiell, J.E., Fett, W.E., and Lundin, C.D. 1977. Technical note: ferrite stability at elevated temperature in austenitic stainless steel weld metal. *Welding Journal*, 56(9):289s–290s.

110. Thomas, R.G. 1978. The effect of delta ferrite on the creep rupture properties of austenitic weld metals. *Welding Journal*, 58(3):81s–86s.

111. Adcock, F. 1926. The effect of nitrogen on chromium and some iron-chromium alloys. *Journal of the Iron and Steel Institute*, 114(2):117–126.

112. Uhlig, H.H. 1942. The role of nitrogen 18-8 stainless steel. *Trans. ASM* 34:947–982, December.

113. Franks, R., Binder, W.O., and Thompson, J. 1955. Austenitic chromium-manganese-nickel steels containing nitrogen. *Trans. ASM* 47:231–266.

114. Zackay, V.F., Carlson, J.F., and Jackson, P.L. 1956. High nitrogen austenitic Cr-Mn steels. *Trans. ASM* 48:508–525.

115. Whittenberger, E.J., Rosenow, E.R., and Carney, D.J. 1957. Elevated temperature phase relationships in the Cr-Ni-Mn-N system. *Journal of Metals*, 9:889–895, July.

116. Gunia, R.B., and Woodrow, G.R. 1970. Nitrogen improves engineering properties of chromium-nickel-stainless steel. *Journal of Materials*, 5(2):413–430.

117. Espy, R.H. 1982. Weldability of nitrogen-strengthened stainless steels. *Welding Journal*, 61(5):149s–156s.

118. Erasmus, L.A., and Yang, L.J. 1970. Strengthening welds in the warm-worked grades of austenitic stainless steel by the addition of nitrogen to the weld metal. *Welding and Metal Fabrication*, 38(7):269–275.

119. Mel'kumov, I.N., and Topilin, V.V. Alloying austenitic steels with nitrogen. *Metallovedeniei Termicheskaya Obrabotka Metallor*, (3):47–51.

120. Kawabe, Y., and Nakagawa, R. 1971. The effect of interaction of interstitial solute elements on the high temperature strength of 18Cr-18Ni heat resisting steel. *Transactions of National Research Institute for Metals*, 13(5):8–21.

121. Kawabe, Y., Nagawaga, R., and Mukoyama, T. 1970. The effect of nitrogen and molybdenum on the high temperature strength of 18 Cr-12Ni-0.2C austenitic stainless steel. *Transactions of National Research Institute for Metals*, 12(3):15–25.

122. Eckenrod, J.J., and Kovach, C.W. 1979. Effect of nitrogen on the sensitization, corrosion and mechanical properties of 18 Cr-Ni stainless steel. Properties of austenitic stainless steels and their weld metals (influence of slight chemistry variations). ASTM TP 679, eds., Brickman, C.R., and Garvin, H.W. pp. 17–41, American Society for Testing and Materials, Phila., Pa.

123. Baeslack, W.A., Savage, W.F., and Duquette, D.J. 1979. Effect of nitrogen on the microstructure and stress corrosion cracking of stainless steel weld metals. *Welding Journal*, 58(3):83s–90s.

124. Okagawa, R.K., Dixon, R.D., and Olson, D.L. 1983. The influence of nitrogen from welding on stainless steel weld metal microstructures. *Welding Journal*, 62(8):203s–209s.

125. Zhitnikov, N.P., and Zaks, I.A. 1971. Influence of nitrogen in austenitic weld metal structures. *Welding Production*, (8):5–7.

126. Suutala, N. 1982. Effect of manganese and nitrogen on the solidification mode in austenitic stainless steel welds. *Met. Trans.*, 13A(12):2121–2130.

127. Ogawa, T., Aoki, S., Sakamoto, T., and Zaizen, T. 1982. The weldability of nitrogen containing austenitic stainless steel, part 1–chloride pitting corrosion resistance. *Welding Journal*, 61(5):139s–148s.

128. DeLong, W.T., Ostrom, G., Szumachowski, E. 1956. Measurement and calculation of ferrite in stainless steel weld metal. *Welding Journal*, 35(11):526s–533s.

129. Kotecki, D.J. 1978. Welding parameter effects on open-arc stainless steel weld metal ferrite. *Welding Journal*, 57(4):109s–117s.

130. Kobayaski, T., Kuwana, T., and Kikuchi, Y. 1965. Arc atmosphere and nitrogen content of weld metal. *IIW Document XII-265-65.*

131. Arata, Y., Matsuda, F., and Saruwatari, S. 1974. Varestraint test for solidification crack susceptibility in weld metal of austenitic stainless steels. *Trans. of JWRI*, 3:79–88.

132. Molinder, G. 1979. Nickel requirements for equivalent structures in austenitic stainless steel. *Metal Progress*, 86:56–59, November.

133. Pryce, L., and Andrews, K.W. 1960. Practical estimation of composition balance and ferrite content in stainless steels. *Jour. Iron and Steel Institute*, 195:415–417.

134. Sims, C.T., and Hagel, W.C. 1972. Electron hole calculations in superalloys (PHACOMP). *The Superalloys*, pp. 272–283, John Wiley, New York.

135. Woodyatt, L.R., Sims, C.T., and Beattie, Jr., H.J. 1966. Prediction of sigma-type phase occurrence from compositions in austenitic superalloys. *Trans. AIME*, 236:519–527.

136. Parravano, N. 1913. Die Ternaren Legierungen von Eisen-Nickel-Mangan, Nickel-Mangan-Kupfer, Eisen-Mangan-Jupfer. *Int. Zeit. fur Metallographic*, 4:171–202.

137. Rapatz, F. 1939. Austenitic addition material for fusion welding. U.S. Pat. No. 2,156,306.

138. Spraragen, W., and Claussen, G.E. 1937. Welding manganese steels—a review of the literature to July 1. *Welding Journal*, 17(8):1s–22s.

139. Avery, H.S., and Chapin, H.J. 1954. Austenitic manganese steel welding electrodes. *Welding Journal*, 33(5):459–479.

140. Avery, H.S. 1963. Cast heat resistant alloys for high temperature weldments. *Welding Research Council Bulletin 143*, August.

141. Danhier, F. 1953. The weldability of austenitic manganese steels. *Welding Journal*, 28:155s–156s.

142. DeLong, W.T. 1966. Ferrous weld deposit and structure. U.S. Pat. No. 3,266,876.

143. DeLong, W.T., and Reid, Jr., H.F. 1957. Properties of austenitic chromium-manganese stainless steel weld metal. *Welding Journal*, 36(1):1–8.

144. Hochmann, J. 1977. The role of manganese additions in austenite stainless steels. *Materiaux et Techniques*, 65(12):69–87, December.

145. Tavadze, F.N., and Grikurov, G.H. 1983. Processing use and prospects of application of Cr-Mn stainless steels in cryogenic and energy machine construction. Commemoration Book on the 100th Anniversary of the Birth of Academician I.P. Bardin, *IP Bardin and Russian Metallurgy*, Nauka, Moscow, pp. 81–87.

146. Self, J.A., Matlock, D.K., and Olson, D.L. 1984. An evaluation of austenitic Fe-Mn-Ni metal for dissimilar metal welding. *Welding Journal*, 63(9):282s–288s.

147. Andrews, K. 1965. Empirical formulae for the calculation of some transformation temperatures. *JISI*, 203:721–727.

148. Reed, R.P. 1983. Martensitic phase transformations. *Materials at Low Temperatures*, pp. 295–341, ASM, Metals Park, Ohio.

149. Monkman, F.C., Cuff, F.B., and Grant, N.J. 1957. Computation of Ms for stainless steels. *Met. Prog.*, 71:94–96.

150. Eichelmann, G.H., and Hull, F.C. 1953. Effect of composition on the temperature of spontaneous transformation of austenitic to martensitic in 18-8 stainless steel. *Trans. ASM*, 45:77–104.

151. Pugh, J.W., and Nisbet, J.D. 1950. A study of the iron-chromium-nickel ternary system. *Trans. AIME*, 188:268–276.

152. Self, J.A., Olson, D.L., and Edwards, G.R. 1984. The stability of austenitic weld metal. *Proc. of IMCC*, Kiev, USSR, July.

153. Charles, J., and Berghezan, A. 1981. Nickel-free austenite steels for cryogenic applications: the Fe-23%Mn-5%Al-0.2%C alloys. *Cryogenics*, 21(5):278–280.

154. Banerji, S.K. 1978. An austenitic stainless steel without nickel and chromium. *Metal Progress*, 113(4):59–62.

155. Charles, J., Berghezan, A., Lutts, A., and Dancoisne, P.L. 1981. New cryogenic materials: Fe-Mn-Al alloys. *Metal Progress*, 119(5):71–74.

156. Tomaszewicz, P., and Wallwork, G.R. 1984. The oxidation of Fe-Al alloys containing chromium, nickel or manganese. *Corrosion* 40:152–157.

157. Dunning, J.S., Glenn, M.L., and Leavenworth, Jr., H.W. 1984. Substitute for chromium in stainless steel. *Metal Progress*, 126:19–24,

October.

158. Carpenter, B., Olson, D.L., and Matlock, D.K. 1985. A diagram to predict aluminum passivated stainless steel weld metal microstructure. Presented at the 1985 AWS 66th Annual Convention, Las Vegas, Nevada, April.

159. Liu, S., Matlock, D.K., and Olson, D.L. 1985. A thermodynamic and kinetics approach in the development of expressions for alloy behavior prediction. Colorado School of Mines, in preparation.

160. Kaufman, L. 1959. The free-energy changes attending the martensitic transformation in the iron-chromium and iron-chromium-nickel systems. *Trans. AIME* (Met. Soc.), 215(4):218–223.

161. Scheil, E. 1942. Benerkungen zur Schichtkristallbildung. *Z. Metallk.*, 34:70–72.

162. Pfann, W.G. 1952. Principles of zone melting. *Trans. AIME*, 194:747–753.

163. Speich, G.R. 1973. Chromium-iron nickel system. *ASM Metal Handbook*, 8th Edition, 8:424–426.

164. Henry, O.H., Claussen, G.E., and Linnert, G.E. 1949. *Welding Metallurgy*. 2nd Edition, AWS, Miami, Florida.

165. Ferree, J.A. 1969. Free machining austenitic stainless steel. U.S. Patent 3,460,939.

166. Avery, H.S. 1974. Heat resistant alloys. U.S. Patent 2,465,780.

167. Lippold, J.C. 1985. Centerline cracking in deep penetration electron beam welds in type 304L stainless steel. *Welding Journal*, 64(5):127s–136s.

168. Flemings, M.C. 1974. *Solidification Processing*. pp. 188–190, McGraw-Hill, New York.

169. Griffith, A.J., and Wright, J.C. 1969. *Mechanical properties of austenitic and metastable stainless steel sheet and their relations with press forming behaviour*. Publication 117, p. 52, Iron and Steel Institute, London, U.K.

WRC Bulletin 305
June 1985

This bulletin contains three summary reports prepared by the Japan Pressure Vessel Research Council (JPVRC) Subcommittee on Hydrogen Embrittlement:

1) "Hydrogen Attack Limit of 2¼ Cr–1 Mo Steel," by Task Group I;
2) "Embrittlement of Pressure Vessel Steels in High Temperature, High Pressure Hydrogen Environment," by Task Group II; and
3) "Hydrogen Embrittlement of Bond Structure Between Stainless Steel Overlay and Base Metal," by Task Group III.

The three Task Group reports were translated and summarized for publication by JPVRC and have been reviewed and edited by the U. S. PVRC Subcommittee on Hydrogen Effects for publication in this bulletin.

The price of WRC Bulletin 305 is $14.00 per copy, plus $5.00 for postage and handling. Orders should be sent with payment to the Welding Research Council, Rm. 1301, 345 E. 47th St., New York, NY 10017.

Call for Papers—
International Welding Research

Papers are solicited for the ASM/AWS/WRC-sponsored conference on "International Trends in Welding Research," to be held in Gatlinburg, Tenn., May 18-22, 1986. This eight-session symposium will cover heat and fluid flow problems in welds, solidification, solid state transformations, mechanical behavior of welds, and welding processes and process control. Conference proceedings will be published. Submit abstracts up to 300 words by November 15, 1985, to S. A. David, Materials Joining Laboratory, Metals and Ceramics Divisions, Oak Ridge National Laboratory, P. O. Box X, Oak Ridge, TN 37831. Inquiries for future information should be addressed to American Society for Metals (ASM) Conference Dept., Metals Park, OH 44073.